

Autocorrelation and crossed-sightline correlation of ECE for measurement of electron temperature and density fluctuations on ATF and TEXT

C. E. Thomas Jr. and R. F. Gandy

Citation: [Review of Scientific Instruments](#) **61**, 3570 (1990); doi: 10.1063/1.1141573

View online: <http://dx.doi.org/10.1063/1.1141573>

View Table of Contents: <http://scitation.aip.org/content/aip/journal/rsi/61/11?ver=pdfcov>

Published by the [AIP Publishing](#)

Articles you may be interested in


[Linear measurement of weak 1.57 \$\mu\text{m}\$ optical pulse train by heterodyne autocorrelation](#)
Appl. Phys. Lett. **69**, 3978 (1996); 10.1063/1.117843

[Autocorrelation function of 1/f current fluctuations in vacuum microelectronics devices](#)
J. Vac. Sci. Technol. B **14**, 2135 (1996); 10.1116/1.588886

[Crossed-sightline correlation of thermal ECE for remote measurement of absolute magnetic fields \(abstract\)](#)
Rev. Sci. Instrum. **63**, 4636 (1992); 10.1063/1.1143641

[Electron temperature fluctuation measurement from ECE on TEXT-U](#)
Rev. Sci. Instrum. **63**, 4633 (1992); 10.1063/1.1143640

[Autocorrelation and crossed-sightline correlation of ECE for measurement of electron temperature and density fluctuations on ATF and TEXT \(abstract\)](#)
Rev. Sci. Instrum. **61**, 3073 (1990); 10.1063/1.1141737

The advertisement for Mad City Labs Inc. (MCL) features a blue background. At the top center is the MCL logo, with 'MCL' in large red letters and 'MAD CITY LABS INC.' in smaller red letters below it. Below the logo are four images of products: a white square nanopositioning stage, a black micropositioning stage, a silver AFM & SPM head, and a black single molecule imaging system. Each image is labeled with its respective name in white text below it.

Nanopositioning Systems

Micropositioning

AFM & SPM

Single molecule imaging

Autocorrelation and crossed-sightline correlation of ECE for measurement of electron temperature and density fluctuations on ATF and TEXT^{a)}

C. E. Thomas, Jr.

Nuclear Engineering Program, Georgia Institute of Technology, Atlanta, Georgia 30332

R. F. Gandy

Department of Physics, Auburn University, Auburn, Alabama 36849

(Received 8 May 1990; accepted for publication 8 June 1990)

The great stumbling block in the quest for fusion power using magnetic confinement devices is anomalous transport. It is conjectured that turbulent plasma fluctuations may be responsible for the degraded energy confinement observed in experiments. There exists a clear need for more detailed experimental studies of plasma microturbulence. A conceptual design is presented for a diagnostic to measure electron temperature and density fluctuations using electron cyclotron emission (ECE). The proposed ECE systems will employ autocorrelation and cross-correlation techniques to measure radiation from the Advanced Toroidal Facility (ATF) at Oak Ridge National Laboratory (ORNL) and also from the Texas Experimental Tokamak (TEXT) at the University of Texas. This set of experiments on a stellarator and a tokamak will allow a unique comparative study of the fluctuation physics in the two different magnetic configurations. This article presents the theoretical basis and conceptual design of the diagnostic.

I. INTRODUCTION

A. Motivation

In the quest for controlled thermonuclear fusion, the magnetic confinement approach has encountered a formidable obstacle: anomalous transport. The experimental values of electron thermal diffusivity exceed those expected from neoclassical theory by orders of magnitude. There clearly exists a lack of understanding of thermal transport in high-temperature plasma devices. It is conjectured that fine-scale plasma microinstabilities may be the cause of the anomalous transport.¹⁻³ Currently no accepted theory exists that can fully explain the experimental results obtained. One of the causes of this lack of understanding is the past experimental emphasis on measuring bulk, time-averaged plasma quantities. In order for the plasma community to understand the basic physics of anomalous transport, experimentalists need to design dedicated plasma diagnostics to measure the fluctuating components of plasma quantities. This is currently being done at many sites.

Electron cyclotron emission (ECE) has the potential to provide information on fluctuations in electron temperature, electron density, and magnetic field. Initially, our experiments will focus on the detection of optically thick, second harmonic ECE to look at fluctuations in electron temperature. Later it is intended to include additional sightlines to allow measurements of fluctuations in electron density and plasma pressure using optically thin emission. We plan a set of experiments to measure fluctuating ECE from the ATF stellarator located at ORNL and TEXT (a moderate sized tokamak) at the University of Texas. This use of a tokamak and a stellarator will lead to insights into the similarities and

differences of transport in the two main classes of toroidal devices.

B. Background

The history of the use of optically thick electron cyclotron emission to measure fluctuations in plasma electron temperature is somewhat of a dichotomy. In the first case, ECE has been used with great success to measure coherent, large amplitude, MHD-type fluctuations (e.g., sawteeth) that have significant spatial extent (> 2 cm) and occur on a relatively slow ($> 10 \mu\text{s}$) time scale. The MHD-related temperature fluctuations are usually localized to a flux surface and can be spatially resolved using the standard ECE diagnostic techniques. References⁴⁻⁶ contain examples of the use of ECE to measure these types of coherent T_e fluctuations. On the other hand, the application of ECE to measure incoherent or turbulent temperature fluctuations has not been at all successful. The only attempt to date did not work because of photon noise limitations.^{7,8} A summary of the present experimental situation would be that coherent, large-scale fluctuations can be easily measured but one should use extreme caution when looking for incoherent, small-scale fluctuations. In the present work we present advanced methods of data analysis using autocorrelation and cross-correlation of ECE to infer turbulent temperature fluctuations.

The clear need for a better understanding of transport in magnetic fusion devices leads one to ask the following question: Can useful information on plasma fluctuations be deduced from ECE? To answer this question one must carefully consider the parameter range of possible T_e fluctuations and the physical limits inherent in a measurement of ECE from a magnetic fusion device. This will be done in Sec. II. In Sec. III the use of cross-correlation and autocorrelation to overcome the traditional limits of ECE physics will be discussed. Then the conceptual design for the diagnostic will be

^{a)} The abstract for this paper appears in the *Proceedings of the 8th Topical Conference on High Temperature Plasma Diagnostics* in Part II, Rev. Sci. Instrum. **61**, 3073 (1990).

discussed in Sec. IV. Finally, the implications of all of the above will be discussed.

II. FLUCTUATION PHYSICS AND PREVIOUS ECE LIMITATIONS

The first step in evaluating the possibility of using ECE to measure T_e fluctuations is to address the nature of these fluctuations. In particular, what level and type of T_e fluctuations are detectable? The answer to this question depends on the spectrum of the fluctuations in $\omega - k$ space and the amplitude of these fluctuations. Obviously we do not have the exact answers, but some limits are set by looking at present and past ECE results. A typical ECE system⁹ used to measure T_e has a spatial resolution of approximately 5 cm and a typical time resolution of 10 μ s. A typical system noise level is of order 5 eV. The lack of evidence of incoherent T_e fluctuations at these levels implies that one needs to look with better spatial resolution, sample at higher frequencies, and reduce the system noise level.

Since no one has yet reported turbulent T_e fluctuations from the interior of a high-temperature plasma, we do not know how much improvement in ECE system performance is required. However we do know that significant improvement in ECE system performance is possible if one designs and dedicates a system to measure fluctuations. As a guide to the type of system performance desired, one can assume that any temperature fluctuations lie in the same part of $\omega - k$ space as the density fluctuations observed to date.¹⁰ With this assumption, one requires a frequency response up to 1 MHz and the ability to resolve wavenumbers in the range of 1–10 cm^{-1} (or wavelengths in the range of 0.5–5 cm). Electron density fluctuation levels on the level of a few percent have been reported. What is required then is an ECE system with the spot size on the order of 1 cm or less, time resolution of 1 μ s or better, and the ability to measure temperature amplitude fluctuations on the order of 1% or less. Of particular interest, in regard to electron temperature fluctuation studies, is the area of trapped electron modes. Recent theoretical work,¹¹ applied to the ATF device, predicts that the trapped electron population will vary greatly for two specific magnetic configurations obtained by varying the quadrupole field. The first configuration is practically shearless on the inner half of the plasma radius, and the second configuration has strong shear throughout. Theory predicts that in the first case the dissipative trapped electron (DTE) mode will be localized and that in the second case it will be extended along field lines. The DTE mode should be more dangerous in the first configuration because of the localization of the drift wave.¹² If these trapped electron modes are the driving cause of anomalous transport, then the effects of varying the trapped electron fraction may be measurable using the fluctuating ECE diagnostic system described herein. It would be exciting to compare scaling laws derived from varying the trapped electron fraction on ATF with the experimental results of ECE measurements on TEXT.

Recent theoretical predictions for mode localization, wavelength, and frequencies have been discussed by Carreras.¹³ For ECH discharges in ATF, it is expected that the maximum fluctuation level for dissipative trapped electron

(DTE) modes will be peaked in the inner third (both sides of the plasma center if orbits are confined) of the plasma radius because of the stellarator low shear. The poloidal wave length is expected to be comparable to the radial width of the mode and is of the order of a few cm. For a tokamak like TEXT, the fluctuation level probably peaks at the half minor radius on the outside (no trapped particles on the inside) with the poloidal wavelength being several times longer than the radial width of the mode and of the order of a centimeter. Contrary to other types of instabilities and because these fluctuations involve trapped electrons, it is expected that the electron temperature fluctuation $\langle \tilde{T}_e/T_e \rangle$ will be larger in comparison to density fluctuations. Frequencies (with no Doppler shift) would be less than 100 kHz. Theoretical predictions of the mode amplitude involve complex nonlinear saturation calculations and are a subject of considerable discussion among plasma theorists.

A. Previous limitations on ECE measurements

Now that we have a guide for the type of ECE system performance required to explore for electron temperature fluctuations, we address the physics limitations of such a system. The critical question to be addressed when assessing the possibility of using ECE to measure electron temperature fluctuations is: What is the minimum achievable spatial resolution? One needs as small a spot size as possible in order to resolve the large wave-number fluctuations associated with the plasma microturbulence. If we consider viewing perpendicularly to the magnetic field, then the spot size for viewing in the horizontal midplane is determined by two factors: (1) transverse spot size set by the diffraction limit, and (2) longitudinal spot size set by frequency linewidth considerations.

Let us first consider the case of viewing the plasma with a horn/lens system that allows focussing in order to minimize spot size in the plasma (see Fig. 1). The spatial extent of the spot width d , transverse to the viewing direction, is determined by the diffraction limit. For the circular aperture case the diameter of the spot is given by the relation $d = 2.44 \lambda f/D$, (where λ = wavelength, f = focal length of the lens, and D = diameter of the lens). This value of d represents the distance between the first two minima in the Airy diffraction pattern and therefore encompasses 84% of the radiated power. Practically the factor f/D , the $f\#$, has a minimum set by the finite size of the vacuum viewing window and lens construction limitations. For the two devices under consideration, these limitations set an $f\#$ minimum of approximately 2. Therefore one finds that $d \geq 5\lambda$. For operation at $B = 2$ Tesla, and second harmonic ECE, this implies that $d_{\min} \approx 1.5$ cm. This result holds for ATF and TEXT. Note that for machines with a higher magnetic field or optically thick higher harmonics the spot size will be even smaller since it scales as B^{-1} .

The second consideration involves the longitudinal extent of the viewing spot size, spatial dimension w in Fig. 1. This dimension is related to the geometry of the surfaces of constant magnetic field magnitude. For the TEXT and ATF cases under consideration (horizontal midplane, viewing toward the center of the plasma), surfaces of constant $|B|$ are

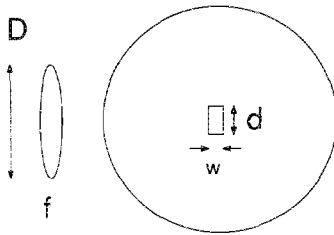


FIG. 1. Definition of ECE spot size. The image spot d is defined by a lens having focal length f and diameter D .

near vertical. For emission perpendicular to the magnetic field the dimension w is set by the natural frequency linewidth convolved with the instrumental bandwidth, which in turn depends on the magnetic field spatial gradient. The lower limit is set by the natural linewidth since the instrumental bandwidth can be set to an arbitrarily low value (while noting that setting the instrumental bandwidth very much lower than the natural linewidth decreases signal without improving spatial resolution). Therefore, we will assume that the instrumental bandwidth is chosen such that the natural linewidth dominates in the determination of dimension w .

The natural line broadening is due to relativistic and/or Doppler broadening depending on the relative angle between the direction of emission and the magnetic field. The spread due to Doppler broadening is minimized by viewing perpendicularly to the magnetic field. Therefore, in our case, the spread is due to relativistic line broadening. For second harmonic ECE the relativistic linewidth is given by¹⁴ $\Delta f/f = 4.1qT_e/m_e c^2$ (where $f = 2f_{ce}$, f_{ce} is the local electron cyclotron frequency, q is the electron charge, T_e is the electron temperature in eV, m_e is the electron mass, and c is the speed of light). The spatial variation of the magnetic field (and therefore of f) then defines w , if the instrumental bandwidth approximately equals the natural linewidth.

The preceding analysis of the determination of the longitudinal extent of the spot size w must be modified when dealing with optically thick harmonics (as is the case for TEXT and ATF at second harmonic, X mode). The reason for this has to do with the reabsorption of radiation that occurs with a blackbody. The effect is illustrated in Fig. 2. Referring to Fig. 2, consider an optically thick emitting layer having a spatial width of w_0 and a total optical depth of τ_0 , where $\tau_0 > 2$. For simplicity, also assume that the absorption coefficient α is constant across the layer. Recall that the optical depth τ is defined as $\int \alpha dx$. Consider radiation emanating from x_0 , toward the receiving horn. As this radiation traverses the layer it will constantly be absorbed and re-emitted with an intensity characteristic of the local electron temperature level. This process will continue as the radiation moves to higher values of x , until the radiation passes a critical value of x , x_{cr} . The point x_{cr} is defined by the characteristic that the accumulated optical depth between x_{cr} and $x = w_0$ is approximately 2 ($\tau = 2$ is chosen as this region will account for approximately 86% of the emission). Therefore, for purposes of viewing the emission from the emitting region, one sees a reduced layer (cross-hatched region) characterized by a smaller, effective width, $w = w_0 - x_{cr}$. The consequences of this effect on the spot size for TEXT and ATF have been calculated for ECE at second harmonic, ex-

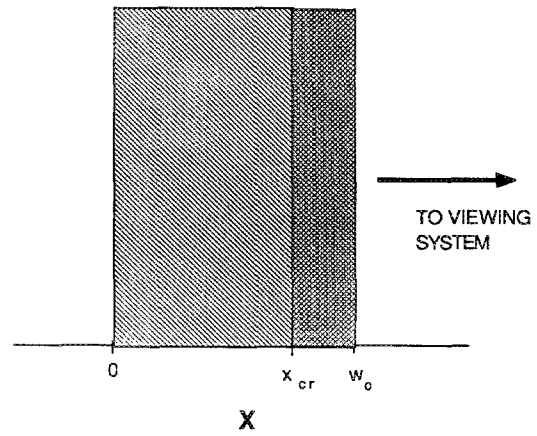


FIG. 2. Optically thick emitting layer having a total optical depth much greater than 2. The effective width of the emitting layer (cross-hatched region) is determined by that part of the volume facing the viewing system that has an optical depth ≈ 2 .

traordinary mode emission where relativistic broadening is the dominant line broadening mechanism. Typical results are shown in Figs. 3 and 4 for ATF and TEXT, respectively. Note that this effect limits w_{min} to a value less than 1 cm for both devices.

Once the spot size has been reduced as much as possible, the next area of concern is the sensitivity of the receiver. For a typical heterodyne receiver the lower limit of the sensitivity is set by the quantum noise limit:¹⁵ $\Delta T_e/T_e \geq (\Delta f_v/\Delta f_r)^{0.5}$. Here Δf_v is the video bandwidth (defined as the inverse of the microwave crystal detector integration time constant) and Δf_r is the bandwidth of the radiation being detected. For a typical radiation bandwidth of 400 MHz and a video bandwidth of 100 kHz this implies that fluctuations in the range of 1%–2% should be detectable. If the observed emission is from plasma regions where $T_e = 100$ to 500 eV, then detection limits of 1–5 eV are possible. Also note the lower levels of sensitivity can be achieved by reducing the video bandwidth (at the expense of time and frequency resolution).

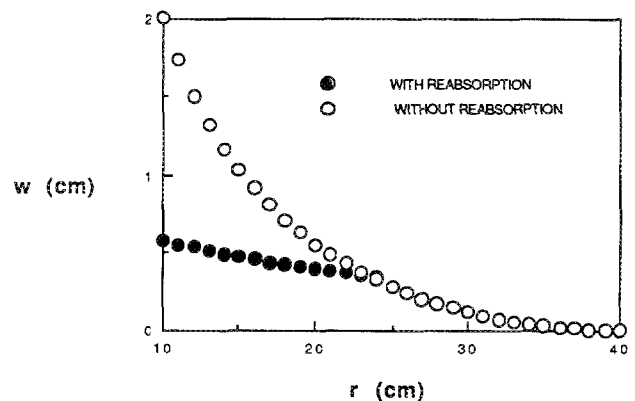


FIG. 3. Second harmonic ECE spatial linewidth dimension w for ATF with $B = 2$ T, $T_{e0} = 1$ keV, and $n_{e0} = 3 \times 10^{13} \text{ cm}^{-3}$. This particular calculation is for vertical (port location) emission and assumes parabolic density and temperature profiles. The results are similar for horizontal (port location) emission. Note that the optical depth equals 2 at approximately 24 cm.

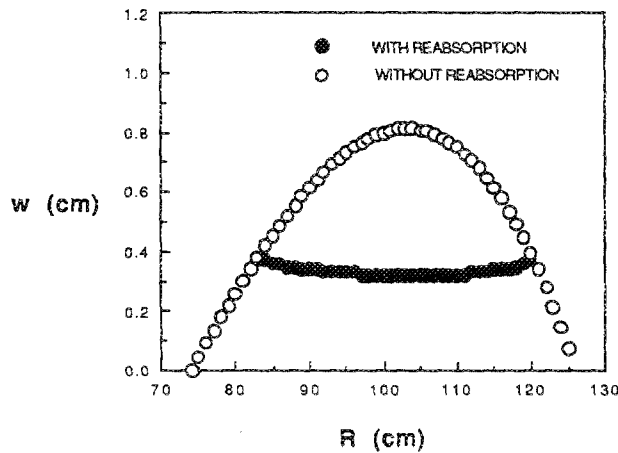


FIG. 4. Second harmonic ECE spatial linewidth dimension w for TEXT with $B = 2$ T, $T_{e0} = 1$ keV, and $n_{e0} = 3 \times 10^{18}$ cm $^{-3}$. This calculation is for horizontal emission and assumes parabolic density and temperature profiles. Note that the optical depth equals 2 at approximately $r = 20$ cm.

One should note that the signal being viewed may depend on magnetic field, temperature, and density. This will depend on which harmonic is being used.

In summary, an ECE diagnostic system using present methods can be optimized to explore a high temperature plasma for T_e fluctuations. The minimum detectable amplitude for fluctuations in the frequency range of interest (order of 100 kHz) is $\sim 2\%$. It will be shown below that this amplitude detection limit can be improved by an order of magnitude with autocorrelation techniques.

III. ECE AUTOCORRELATION AND CORRELATION MEASUREMENTS OF TEMPERATURE AND DENSITY FLUCTUATIONS

A. Introduction

It is our belief that present ECE methods do not give adequate amplitude resolution to measure fluctuations at the frequencies of interest (~ 100 kHz), and give no information about wavelengths of the fluctuation being studied. It has been suggested¹⁶⁻¹⁸ that crossed sightline correlation of ECE would give another method of measuring temperature and density fluctuations. We propose here a variant of that method, auto and cross correlation of a single sightline ECE system, to measure temperature fluctuations including amplitude, frequency dependence, correlation length in the plasma (width in k space), and correlation time (width in ω space). We would like to mention here that Dr. P. Efthimion of PPPL has previously suggested¹⁹ the use of autocorrelation for the measurement of correlation length in the plasma. We have extended our previous work to show that this and considerably more can be measured.

Autocorrelation of an optically thick harmonic must be used to measure temperature fluctuations, as discussed in detail below. If in addition to the sightline for the optically thick harmonic, a crossing sightline for an optically thin harmonic is constructed, then density fluctuations (amplitude, frequency dependence, possibly wavelength dependence) can be measured by comparing the autocorrelation functions

of the two sightlines. Additionally, the PHASE (important for inferring transport) between the density and temperature fluctuations can be inferred by cross correlation of the signal between the two sightlines. It is not presently planned to build the second sightline on either TEXT or ATF. This will be proposed at a later date after demonstration of the temperature fluctuation measurement.

It is demonstrated below that the resolution of the autocorrelation system is limited only by the integration time available. The maximum time for integration is limited by the amount of time that an experiment is in a quasi steady state. On TEXT and ATF this time period is from 10 to 100 ms. For this integration time we estimate that the proposed ECE autocorrelation diagnostic can resolve temperature fluctuations of $2 \times 10^{-3} T_e$, i.e., 0.2%, at frequencies of 100 kHz. This is an order of magnitude better than the resolution of a traditional heterodyne ECE system. The frequency resolution would be on the order of 1 kHz, and the diagnostic will be responsive to wavelengths longer than 1 cm, and will give the spread in k space of the wavelengths for each frequency band measured. For machines with higher magnetic fields or temperatures, it may be possible to achieve sensitivity to fluctuation wavelengths of the order of 1 mm, since higher magnetic field and higher harmonics means smaller spot sizes for the antenna pattern, and higher temperature and density implies greater optical depth and a corresponding decrease in the emission line width.

There is of course some price to pay for the improved resolution of the autocorrelation ECE diagnostic. In this case it is not money (the diagnostic is relatively cheap) so much as time resolution. It is necessary to assume that the average amplitude of the turbulent fluctuations is constant over the time period of the integration. Since the integration period is restricted to a length of time such that the experiment is "steady state," we believe that this is a reasonable assumption. Note that this does not restrict the frequency resolution of the diagnostic, only the time resolution of the average turbulent amplitude at a particular frequency.

B. Correlation functions defined

Figure 5 shows the conceptual optical design of the diagnostic and Fig. 6 shows the electronics. The design of the sightline in this diagnostic is very similar to the design of the ECE diagnostic on ATF.²⁰ The received signal at the an-

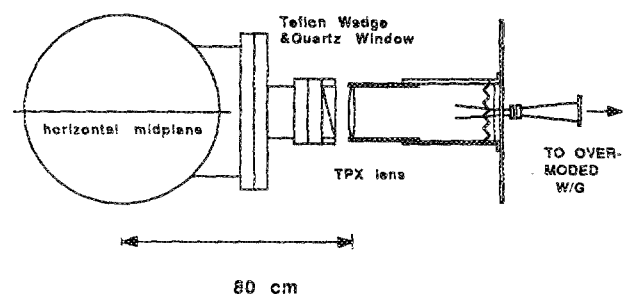


FIG. 5. Proposed setup of the ECE viewing system on ATF showing vacuum window, lens, horn, and transition to overmoded waveguide.

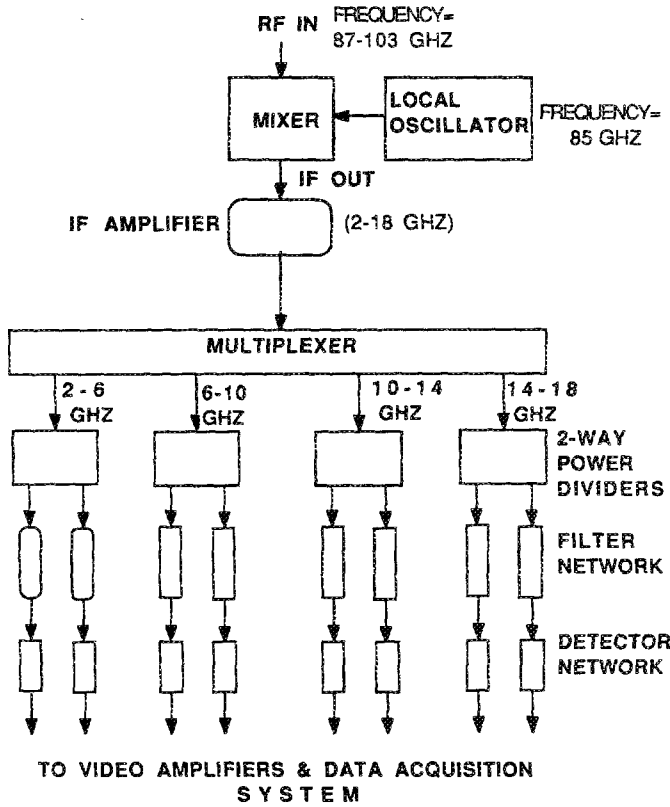


FIG. 6. Proposed setup of the ECE receiver system on ATF showing mixer, local oscillator, IF amplifier, multiplexer, power dividers, filter network, and detectors.

tenna (as described in more detail below) will be bandpass filtered into two identical passbands $\delta\omega_i$ about several frequencies ω_i at time t and $t + \tau$ and fed into microwave detectors. The two signals thus derived for each ω_i are identical except that one is delayed with respect to the other by a time τ . The delay must be achieved in hardware (to be demonstrated in Sec. III H), and the purpose of the delay will be described in detail below. Basically it makes the quantum fluctuations (thermal fluctuations) of the two signals incoherent with respect to one another, but leaves the bulk plasma fluctuations still coherent (correlated). Let the signal out of these detectors due to emission along the sightline be described by $I(\omega_i, t)$ and $I(\omega_i, t + \tau)$ for detectors 1 and 2, respectively, where ω_i is the center frequency of the i th double-channel of the detector array. For a turbulent plasma, the signal I will have a steady-state part \bar{I} and a fluctuating part i , in which case

$$I(\omega_i, t) = \bar{I}(\omega_i) + i(\omega_i, t). \quad (1)$$

The steady-state part of I is given by the mean value,

$$\bar{I}(\omega_i) = \frac{1}{T} \int_0^T I(\omega_i, t) dt, \quad (2)$$

where T is the averaging time. Note that I can be electronically high pass filtered to remove \bar{I} , or this can be done in software.

The correlation function is defined as²¹

$$R_{lk}(\tau) = \lim_{T \rightarrow \infty} \frac{1}{T} \int_0^T i_l(t) i_k(t + \tau) dt, \quad (3)$$

where R_{lk} is precisely the cross-correlation function (CCF) if i_l and i_k have mean values of zero, and again T is the averaging or correlation time. The autocorrelation function (ACF) is defined as the special case when $l = k$. For the single sightline of this diagnostic, the cross-correlation function is estimated by

$$R_{ij}(\omega_i, \omega_j, t, \tau) = \frac{1}{T} \int_{-T/2}^{T/2} i(\omega_i, t + \xi) i(\omega_j, t + \xi + \tau) d\xi \\ = \langle i(\omega_i, t) i(\omega_j, t + \tau) \rangle, \quad (4)$$

where $\langle \rangle$ is defined as the time correlation function operator, T is a finite period, and we also allow for the possibility of cross-channel correlation; i.e., the ECE signal at frequency ω_i is correlated with the ECE signal at frequency ω_j . This has many of the characteristics of cross-correlation since looking at different ECE frequencies corresponds to looking at different spatial locations. Therefore, for ω_i not equal to ω_j , it will be described as cross correlation.

If j is defined as the local value of the fluctuating part of the emission at positions s along the sightline, that is,

$$j(\omega_i, s, t) = \frac{di}{ds}, \quad (5)$$

then Eq. (4) can be written as

$$R_{ij}(\omega_i, \omega_j, t, \tau) = \left\langle \int ds_1 \int ds_2 j(\omega_i, s_1, t) j(\omega_j, s_2, t + \tau) \right\rangle. \quad (6)$$

The region in a plasma where ECE of frequency ω_i is emitted is limited to regions where the cyclotron harmonic is approximately equal to ω_i . The width of this region is the smaller of the natural line width or the absorption length at that point in the plasma, so that

$$R_{ij}(\omega_i, \omega_j, t, \tau) \\ = \int_{r(\omega_i) - l_c}^{r(\omega_i) + l_c} ds_1 \int_{r(\omega_j) - l_c}^{r(\omega_j) + l_c} ds_2 \langle j(\omega_i, s_1, t) j(\omega_j, s_2, t + \tau) \rangle, \quad (7)$$

where $r(\omega_i)$ is the point of peak emission of the received signal at frequency ω_i (not the same as the point of peak emission for an optically thick harmonic), the distance l_c is the smaller of the absorption length (optical depth) or natural linewidth, and the time operator has been passed through the two spatial integrals. The above integral can be approximated as

$$R_{ij}(\omega_i, \omega_j, t, \tau) = (2l_c)^2 \langle j[\omega_i, r(\omega_i), t] j[\omega_j, r(\omega_j), t + \tau] \rangle. \quad (8)$$

C. Autocorrelation time of thermal emission

It can be shown²² that the autocorrelation time of a steady-state thermal source of radiation (i.e., one without macroscopic turbulent fluctuations) is given by

$$\tau_c = 2\pi/\delta\omega_i, \quad (9)$$

where $\delta\omega_i$ is the radian frequency passband width, full width at half maximum (FWHM), of the filter in the channel used to look at the source, and it is assumed that the source is broad-band compared to the filter. This means that the sta-

tistical (quantum) fluctuations of a thermal source are 100% correlated with themselves for times short compared to τ_c . This would appear to prevent autocorrelation from being used as a method of measuring the turbulent fluctuations of a plasma, since in most cases of interest the quantum fluctuations are larger than the turbulent fluctuations of interest. However, it is straightforward to resolve this problem. For passband frequency widths $\delta\nu \gg 100$ MHz, the quantum correlation time is less than 10 ns. However, the turbulent frequency fluctuations of interest have timescales of the order 1 ms to 1 μ s. Thus if the autocorrelation signal in one of the dual paths is delayed by ~ 10 ns, then the quantum fluctuations will be uncorrelated and their auto or cross correlation will go to zero, but the turbulent fluctuations remain 100% correlated with themselves. This allows autocorrelation to separate the quantum (thermal) fluctuations from the turbulent fluctuations, and explains why we have used the unequal time correlation function $R_{ij}(\tau)$ above, and will continue to use it below. A slightly more sophisticated treatment of this problem including the effect of the microwave crystal detector time constant (which forces the required delay in hardware, rather than software) will be given in Sec. III H below.

D. Uncertainty in the correlation function

The variance of the calculated cross-correlation function of $i(\omega_i, t)$ and $i(\omega_j, t + \tau)$ for identical bandwidths, Δf , is²¹

$$\sigma_{ij}^2 = (1/2\Delta f T) [R_{ii}(0)R_{jj}(0) + R_{ij}^2(\tau)], \quad (10)$$

where T is the correlation integration time of $i(\omega_i, t)$ and $i(\omega_j, t + \tau)$ in Eq. (4), σ_{ij}^2 is the variance of $R_{ij}(\tau)$, Δf is the effective bandwidth, and $R_{ij}(\omega_i, \omega_j, t, \tau)$ has been previously defined. For convenience we will often shorten $R_{ij}(\omega_i, \omega_j, t, \tau)$ to $R_{ij}(\tau)$. The requirement that $\Delta f T \gg 5$ is used in obtaining this equation.

The uncertainty in $R_{ij}(\tau)$ is estimated from (also from Ref. 21)

$$\epsilon^2 \equiv \frac{\sigma_{ij}^2}{R_{ij}^2(\tau)} = \frac{1}{2\Delta f T} (1 + \rho_{ij}^{-2}), \quad (11)$$

where

$$\rho_{ij}(\tau) = \frac{R_{ij}(\tau)}{\sqrt{R_{ii}(0)R_{jj}(0)}} \quad (12)$$

is the cross-correlation coefficient function. Equation (11) can be rewritten as

$$\sigma_{ij} = R_{ij}(\tau) \left(\frac{1 + \rho_{ij}^{-2}}{N} \right)^{1/2}, \quad (13)$$

where N is the number of data points used in calculating $R_{ij}(\tau)$. See Bendat and Piersol²¹ for the derivation of Eq. (13). The uncertainty in the autocorrelation function is found by using the above equations with subscripts ij replaced by ii .

The signals $i(\omega_i)$ and $i(\omega_j)$ can be written as

$$i(\omega_i, t) = s(t) + m(\omega_i, t) \quad (14)$$

and

$$i(\omega_j, t) = s(t) + n(\omega_j, t), \quad (15)$$

where $s(t)$ is the correlated emission, and $m(\omega_i, t)$ and $n(\omega_j, t)$ are uncorrelated emission (noise for our purposes). For this diagnostic $\langle m^2 \rangle$ and $\langle n^2 \rangle$ are probably due to equivalent physical phenomena. In this case, they can be treated as equivalent but uncorrelated noise sources, i.e., $\langle n^2 \rangle = \langle m^2 \rangle$. Substituting these relations into the equation for the cross-correlation coefficient produces the desired result,¹⁸

$$\rho_{ij} = \frac{1}{1 + (\langle n^2 \rangle / \langle s^2 \rangle)}. \quad (16)$$

E. Expected line shape

The expected line shape of the cross-correlation function $R_{ij}(\delta\omega_{ij}, t, \tau)$ versus frequency difference $\delta\omega_{ij} = |\omega_i - \omega_j|$ is difficult to calculate as it depends on the natural spatial linewidth (l_{ns}) of the ECE, the correlation length (l_c), and correlation function shape in the plasma, the spot size of the antenna sightline w , the absorption length (optical depth) l_a , and the wavelength of the fluctuation being measured. It is quite probable that the cross-correlation function will have a Gaussian distribution. This statement is supported by the *central limit theorem*,²¹ which asserts that the Gaussian distribution will result quite generally from the sum of a large number of independent random variables acting together. Assuming the turbulent modes in the plasma are independent, the Gaussian shape follows.

It is assumed that the sightline will be arranged perpendicular to the magnetic field so that the natural line width will be due to relativistic broadening of the emission. In general, the requirement of perpendicularity is relaxed to requiring that the Doppler broadening be less than the relativistic broadening. This allows for some deviation from true perpendicularity of the sightlines to the magnetic field. The natural line width $\delta\omega_n$ (full width at half maximum) due to relativistic broadening is given by¹⁴

$$\frac{\delta\omega_n}{s\omega_b} = c_s \left(\frac{v_{te}}{c} \right)^2, \quad (17)$$

where ω_b is the fundamental cyclotron frequency, and v_{te} is the electron thermal velocity [but is defined as $v_{te} = (T/m)^{1/2}$ rather than the often used $(2T/m)^{1/2}$]. Here s is the harmonic number, and c_s is a constant that changes with harmonic number, e.g. for $s = 3$, $c_s = 4.8$.

We have also calculated line broadening due to the Doppler shift caused by the finite angular spread of a Gaussian beam, and the line broadening due to finite transit-time effects. Our calculations show that both of these are much less than the relativistic broadening.

To calculate the variance in frequency space of $R_{ij}(\delta\omega_{ij}, \tau)$, it is assumed that the two dominant factors are the correlation length and the emission linewidth. If the natural ECE linewidth in frequency space is considered as its equivalent spatial linewidth,

$$l_{ns} = \frac{B}{\nabla B} \frac{\delta\omega_n}{s\omega_b} = Rc_s \left(\frac{v_{te}}{c} \right)^2, \quad (18)$$

then the variance is approximated by

$$\delta\omega_c^2 = (\omega_i^2/R^2)(l_c^2 + l_e^2), \quad (19)$$

where again we take the emission linewidth l_e as the smaller of l_{ns} or l_a . Then $\delta\omega_c$ is the width (FWHM) in frequency space of the cross-correlation function $R_{ij}(\delta\omega_{ij}, t, \tau)$, ω_i is the approximate cyclotron harmonic frequency under consideration, and R is the average major radius of $r(\omega_i)$ and $r(\omega_j)$. Note that this defines the correlation function in frequency space,

$$R_{ij}(\delta\omega_{ij}, t, \tau) = R_{ii}(\omega_i, \tau) \exp \left[-\frac{1}{2} \left(\frac{\omega_i - \omega_j}{\delta\omega_c} \right)^2 \right]. \quad (20)$$

Once $\delta\omega_c$ and $R_{ii}(\omega_i, \tau)$ are calculated, a continuous Gaussian distribution for $R_{ij}(\delta\omega_{ij}, t, \tau)$ is defined. For our experiments we will measure $R_{ij}(\delta\omega_{ij}, t, \tau)$ vs $\delta\omega_{ij}$ [including $R_{ii}(\omega_i, \tau)$].

F. Estimating the correlation noise

The next step is to estimate the uncertainty in each value $R_{ij}(\delta\omega_{ij}, t, \tau)$ using Eq. (13),

$$\sigma_{ij} = R_{ii}(\omega_i, t, \tau) \left(\frac{1 + \rho_{ij}^{-2}}{N} \right)^{1/2}. \quad (21)$$

The cross-correlation coefficient ρ_{ij} is calculated using Eq. (16). To do this, we must estimate the sources of the noise $\langle n^2 \rangle$. The uncorrelated signal (noise) can be divided into two categories: noise produced in the plasma and noise produced in the microwave hardware. If we approximate the hardware noise (after the IF amp) as 0.01-eV black body emission, our ECE power calculations for *TEXT* and *ATF* show the hardware noise to be down by at least four orders of magnitude relative to the signal, and we find that plasma noise dominates.

The remaining noise can be divided into three sources: the quantum noise at the detectors, the uncorrelated signal incident on the antenna due to reflections off the vacuum vessel (optically thin harmonics only), and uncorrelated emission along the sightline.

Radiometer theory¹⁵ has shown that for thermal emission the fluctuation about the average signal value is given by

$$n_q = \frac{S_T}{\sqrt{\tau_d \delta\omega_i / 2\pi}}, \quad (22)$$

where n_q is the quantum noise, S_T is the total average received signal, $\delta\omega_i$ is the bandwidth of the channel (previously defined), and τ_d is the microwave crystal detector integration time. The total average received signal is defined as the dc signal plus vacuum vessel reflections. This can be written as

$$S_T = \bar{I} + Q\bar{I}(1 - \eta), \quad (23)$$

where \bar{I} is as before, Q is the cavity resonance term for the vacuum vessel, and η is the viewing dump efficiency (absorption coefficient). For optically thick harmonics, $\eta = 1$. The vacuum vessel cavity resonance is defined as

$$Q = 1/(1 - R_w), \quad (24)$$

where R_w is the wall reflectivity of the vacuum vessel.

To calculate the correlation coefficient ρ_{ij} , the noise terms must be normalized to the correlated signal $s(\delta\omega_{ij}, t)$ [see Eq. (16)]. Thus the normalized quantum noise can be written as

$$\frac{n_q}{s(\delta\omega_{ij}, t)} = \frac{1 + Q(1 - \eta)}{A_f \sqrt{\tau_d \delta\omega_i / 2\pi}}, \quad (25)$$

where A_f is the emission fluctuation due to correlated fluctuations in density, temperature, or magnetic field and is defined as

$$\begin{aligned} A_f &\equiv \frac{s(\delta\omega_{ij}, t)}{\bar{I}} \\ &\approx \frac{1}{\bar{I}} \left\{ R_{ii}(\omega_i, \tau) \exp \left[-\frac{1}{2} \left(\frac{\omega_i - \omega_j}{\delta\omega_c} \right)^2 \right] \right\}^{1/2} \\ &= A_{f0} \exp \left[-\frac{1}{4} \left(\frac{\omega_i - \omega_j}{\delta\omega_c} \right)^2 \right], \end{aligned} \quad (26)$$

and A_{f0} is defined as the emission fluctuation fraction at ω_i . The second equality above follows by using Eq. (20) as $\langle s^2 \rangle$ and approximating $s^2(t) \approx \langle s^2 \rangle$.

For optically thick sight lines and assuming $l_e \gg l_c$ we neglect the other two sources of noise.

G. Autocorrelation measurements of temperature fluctuations

Having done the heavy work, it is now easy to show how to use autocorrelation of ECE to measure temperature fluctuations, and calculate the expected resolution of the measurement. For optically thick plasmas, the ECE emission is given by the low-frequency limit of the black body radiation law $I \propto \omega^2 T_e$. Thus Eq. (4) becomes

$$\begin{aligned} R_{ij}(\omega_i, \omega_j, t, \tau) &= k^2 \omega_i^2 \omega_j^2 \langle \tilde{T}_e[r(\omega_i)] \tilde{T}_e[r(\omega_j)] \rangle, \end{aligned} \quad (27)$$

where k^2 is an appropriate constant (easily calculated), and all the other symbols have been previously defined. The reader is reminded that $r(\omega_i)$ is the spatial point of maximum received emission on the sightline of the detected ECE signal at frequency ω_i . Then for $i = j$ this becomes the autocorrelation function

$$R_{ii}(\omega_i, t, \tau) = k^2 \omega_i^4 \langle (\tilde{T}_e[r(\omega_i)])^2 \rangle, \quad (28)$$

and it is immediately obvious that $R_{ii}(\tau)$ is proportional only to the temperature fluctuations, since we choose τ so that the quantum fluctuations are uncorrelated, and the system is designed so that the correlated system noise is less than the expected turbulent fluctuation amplitude.

The next question of interest is the resolution of the measurement of \tilde{T}_e . Assuming that the emission is optically thick (so that the "viewing dump noise") can be ignored, and also assuming that the correlation length is longer than the effective spatial emission linewidth, then Eq. (22) and Eq. (26) can be used in Eq. (21) to give the expression for the uncertainty:

$$\epsilon = \frac{\sigma_{T_c}}{\bar{T}_c} = \frac{\sigma_{ii}}{2R_{ii}(\tau)} = \frac{1}{2} \left(\frac{2 + [1/(f\tau_d)^2 A_{f0}^4]}{\nu_d T} \right)^{1/2}, \quad (29)$$

where $f = \delta\omega_i/(2\pi)$ is the ECE channel bandwidth (~ 400 MHz), τ_d is still the detector time constant, A_{f0} is normalized electron temperature fluctuation amplitude \bar{T}_e/T_e (assumed $\geq 2 \times 10^{-3}$), ν_d is the data acquisition rate (~ 1 MHz), and T is the integration time. Setting $\epsilon \leq 1$ and solving for T gives $T \geq 5$ ms, where we set $\nu_d = 2/\tau = 200$ kHz so that we can resolve fluctuations at 100 kHz. Note that the data can be smoothed and bandpass filtered in software, before it is correlated, for frequencies less than the actual physical data acquisition rate (thus justifying using $\nu_d = 200$ kHz). Also, if the effective data rate is averaged to 200 kHz, then the effective detector time constant is increased by the smoothing, so that $\tau_d = 10 \mu\text{s}$. This demonstrates the advertised amplitude resolution of the measurement. The resolution in frequency space is limited only by our ability to smooth and filter the data in software for frequencies up to the Nyquist frequency $\nu_d/2$.

The correlation length in the plasma is inferred from the cross-channel correlation function measurements discussed above [Eq. (20)], and the time correlation (frequency width) of the turbulence is estimated by calculating $R_{ii}(\tau)$ from the data for a range of τ 's greater than the quantum autocorrelation time and taking the measured τ_c for the turbulence to be the FWHM of $R_{ii}(\tau)$.

H. Effects of finite detector time constant

In Sec. III B it was mentioned that a finite detector time constant (i.e., the microwave crystal detector time constant for each frequency channel) affects the autocorrelation of signals with self-correlation times shorter than the detector time constant τ_d (e.g., thermal correlation). The basic result is that the signals remain correlated at a low level for times considerably longer than would be inferred from the autocorrelation time of the signal before detection. The derivation of the required results is nicely presented by Loudon,²² and only the final equations are given here. He shows that the intensity–intensity correlation function of the fluctuations of an electromagnetic signal due to thermal emission (thermal linewidth with a Gaussian shape) is given by

$$\langle i_1(t)i_2(t+\tau) \rangle / \bar{I}_1 \bar{I}_2 = [g_2(\tau) - 1] = \exp(-\delta^2 \tau^2), \quad (30)$$

where the incident beam is split into two channels, one which is instantaneously detected i_1 , and the other i_2 which is delayed by increasing the detector distance from the splitter. The time delay is τ as before, and $\delta = \delta\omega_i/(1.18)$, where $\delta\omega_i$ is the FWHM in frequency space of the channel, also as before. The variables \bar{I}_1 and \bar{I}_2 are previously defined as the average dc signal for each channel. The function $[g_2(\tau) - 1]$ is Loudon's notation for the correlation function and is provided to assist the interested reader in locating the derivation.

It can be similarly shown that for a Lorentzian line

shape with FWHM γ that the intensity–intensity correlation function is given by

$$\langle i_1(t)i_2(t+\tau) \rangle / \bar{I}_1 \bar{I}_2 = [g_2(\tau) - 1] = \exp(-2\gamma\tau), \quad (31)$$

where for convenience we assume that τ is positive (i.e., $t_2 \geq t_1$).

Both of the above equations were derived under the assumption that the detector had infinitely fast time response ($\tau_d = 0$). For the case of a finite detector integration time τ_d , the correlation function must be convolved over the detector's memory of past signals with the detector response function of each detector. Loudon derives the finite detector time constant form of the intensity–intensity correlation function for a delay time between the two detectors $\tau = 0$. Unfortunately our problem is to make the thermal correlations disappear by using a finite delay $\tau = t_2 - t_1$, where t_1 is the signal correlation time at the first detector, t_2 is the signal correlation time at the second detector, and for convenience we again assume $t_2 \geq t_1$. Therefore, following Loudon's lead, the intensity–intensity correlation function allowing for a finite detector time constant τ_d and for a delay τ between the two signals, is given by

$$\begin{aligned} \frac{\langle i_1(t)i_2(t+\tau) \rangle}{\bar{I}_1 \bar{I}_2} &= \frac{1}{\tau_d^2} \int_{-\infty}^{t_1} du \left[\int_{-\infty}^{t_2} dv \exp(-2\gamma|v-u|) \right. \\ &\quad \left. \times \exp\left(-\frac{(t_1-u)}{\tau_d}\right) \exp\left(-\frac{(t_2-v)}{\tau_d}\right) \right], \end{aligned} \quad (32)$$

where we have convolved the exponentially decaying detector time responses with (for convenience) the Lorentzian form of the intensity–intensity correlation function since the final result depends little on the exact line shape. Evaluating this rather horrible (for an experimentalist) integral leads to:

$$\begin{aligned} \frac{\langle i_1(t)i_2(t+\tau) \rangle}{\bar{I}_1 \bar{I}_2} &= \frac{1}{2\gamma\tau_d^2} \left[\left(\frac{\gamma\tau_d^2}{2\gamma\tau_d + 1} \right) \exp\left(-\frac{\tau}{\tau_d}\right) \right. \\ &\quad \left. + \left(\frac{\gamma\tau_d^2}{2\gamma\tau_d - 1} \right) \exp\left(-\frac{\tau}{\tau_d}\right) \right. \\ &\quad \left. - \left(\frac{\gamma\tau_d^2}{4\gamma^2\tau_d^2 - 1} \right) \exp(-2\gamma\tau) \right]. \end{aligned} \quad (33)$$

For the case of interest where $\tau \gg \tau_d \gg (1/\gamma)$, this simplifies to:

$$\frac{\langle i_1(t)i_2(t+\tau) \rangle}{\bar{I}_1 \bar{I}_2} = \frac{1}{2\gamma\tau_d} \left[\exp\left(-\frac{\tau}{\tau_d}\right) \right]. \quad (34)$$

The expected correlation due to turbulent temperature fluctuations is given by

$$\frac{\langle i_1(t)i_2(t+\tau) \rangle}{\bar{I}_1 \bar{I}_2} = A_{f0}^2 \left[\exp\left(-\frac{2\tau}{\tau_c}\right) \right]. \quad (35)$$

Since we expect the temperature fluctuation correlation time to be much longer than the detector time constant, $\tau_c \gg \tau_d$, and where for simplicity in evaluation of the next equation

below a Lorentzian line shape has been assumed rather than the Gaussian line shape we actually expect. The next conclusion remains the same with either line shape. Here A_{f_0} is the normalized electron temperature fluctuation fraction, and $\tau_c = 1/\delta\omega_c$ is the self-correlation time of the turbulent temperature fluctuations as previously defined.

Requiring that the ratio of the thermal correlation to the turbulent correlation be less than r_1 , where $r_1 \ll 1$, leads to the following inequality for the required correlation delay time τ :

$$\tau \geq \frac{\tau_d}{1 - (\tau_d/\tau_c)} \times [-\ln(\gamma) - \ln(2\tau_d) - 2\ln(r_1 A_{f_0})]. \quad (36)$$

Further requiring in inequality (36) that $(\tau/\tau_c) = r_2$, where $r_2 \ll 1$ is also required (so that the delay to decorrelate the thermal fluctuations does not decorrelate the turbulent fluctuations), leads to a constraint on the detector time response:

$$\tau_d \leq \frac{r_2 \tau_c}{[r_2 - \ln(\gamma) - \ln(2\tau_d) - 2\ln(r_1 A_{f_0})]}. \quad (37)$$

Inserting reasonable values for the parameters ($r_2 = r_1 = 0.1$, $A_{f_0} = 2 \times 10^{-3}$, $\gamma = 400 \times 10^6$ MHz, $\tau_c = 10^{-5}$ s), and iteratively solving for τ_d quickly leads to the conclusion that the data acquisition rate ν_d must be greater than 10 MHz. This follows because our derivation of the signal to noise ratio for the \tilde{T}_e measurement requires $\nu_d \approx (1/\tau_d)$. This kind of data acquisition rate is not only expensive (for the ADCs, fast detectors, and memory) but leads to unwieldy amounts of data when the acquisition time is stretched over tens to hundreds of milliseconds. It follows immediately then that the delay time between channels to decorrelate the thermal emissions should be introduced in the microwave hardware so that Eq. (31) applies, and the data acquisition rate can be in the more reasonable range of $\nu_d \approx 1$ MHz.

I. Required hardware delay time τ_h

Since it is still required that the hardware delay time τ_h be long enough that the correlation of thermal fluctuations be much less than the turbulent correlation, the ratio of Eq. (31) and Eq. (35) can again be set to r_1 , $r_1 \ll 1$, and solved to give a value for the required hardware (waveguide) time delay:

$$\tau = \frac{-\ln(r_1 A_{f_0})}{2\Delta f_r}, \quad (38)$$

where all quantities are previously defined and Δf_r is the FWHM of the microwave passband filter just in front of each microwave crystal detector, as before. If different filter passbands are used then either different delays must be used or the delay must be calculated using the smallest Δf_r . Using reasonable values for the parameters ($r_1 = 0.1$, $A_{f_0} = 2 \times 10^{-3}$, and $\Delta f_r = 400 \times 10^6$) gives $\tau = 20$ ns. This means a waveguide delay of 20 ns must be introduced after the spatial signal is split in hardware, and before the microwave crystal detectors.

J. Allowable correlated electronic noise

The noise temperature of any correlated electronic noise must be much less than the signal we hope to detect. If the minimum local electron temperature looked at is 100 eV, and $A_{f_0} = 2 \times 10^{-3}$ is to be resolved, then the allowable correlated noise should be an order of magnitude smaller, $n = 0.02$ eV. This will define where the incoming signal must be split. One very convenient place to split the signal and delay one side would be after the LO/mixer and IF amps. In this case the total noise temperature of the system up to the splitter must be less than 0.02 eV.

K. Effect of optical thickness

For a finite optical depth, we require that the signal from turbulent fluctuations reflected off the vessel wall into our viewing system be small compared to the local fluctuation signal. The net reflected signal into the viewing system is

$$s = \frac{i}{1 - R_w e^{-\tau}} e^{-\tau}, \quad (39)$$

where i is the signal emitted along the sightline, as before, R_w is the wall reflectivity, and τ is now the previously discussed optical depth (rather than the time delay). Since we require $s/i = r_1$, where $r_1 \ll 1$, the equation can be solved for τ :

$$\tau = \ln\left(\frac{1 + r_1 R_w}{r_1}\right). \quad (40)$$

For typical parameters ($r_1 = 0.1$, $R_w = 0.90$), we require that the optical depth be $\tau \geq 2.4$. For optical depths less than this there must be a viewing dump on the far wall.

L. Effect of local oscillator frequency stability

If the local oscillator (LO) used to mix the received ECE radiation down to an intermediate frequency is not absolutely constant in frequency, the frequency width of δf of the LO will appear to be a temperature fluctuation (this assumes that a single LO is used for the immediate frequency channel and the delayed frequency channel). It can be shown that the apparent temperature fluctuation is given by

$$\tilde{T}_e = \frac{\delta f}{f} \frac{T_e}{\epsilon}, \quad (41)$$

where ϵ is the inverse toroidal aspect ratio r/R , and all other symbols are previously defined. This sets an easily calculable limit on the required frequency stability of the LO, if a single LO per spatial sightline design is used.

M. Effect of true magnetic field fluctuations

True ripple of the toroidal field or helical field of a toroidal device always exists at some level, since no power supply is perfect. Fortunately these ripples are at frequencies generally less than 1 kHz, so they are expected to be in the region high pass filtered out by the data acquisition system. Because the ECE emission is proportional to B^2 , the apparent temperature fluctuation caused by any such ripple will render that portion of the fluctuation spectrum unusable.

IV. CONCEPTUAL DESIGN

We intend to perform a set of experiments on ATF and TEXT to measure second harmonic, extraordinary mode, optically thick, fluctuating ECE during 2-Tesla operation. Using as small a spot size as possible, we will look for fluctuations from a given spot in the plasma. We will cross correlate two or more different emission frequencies from the same sightline to look for fluctuations. The use of two or more channels has an additional advantage because one can in principle deduce the radial wave-vector range δk_r of the fluctuations by finding the e^{-1} distance of the correlation function by measuring the correlation function versus channel separation. The capability to look for time-correlation information from a single point will be provided by dividing the signal in hardware, time delaying part of it (in hardware), and then autocorrelating the two signals. The signal for a particular ECE frequency is split in hardware rather than software to provide for improved noise rejection (rejection of thermal correlation by hardware delay is discussed in Sec. III H). Random noise added at any hardware stage in the frequency range of interest would be 100% correlated if the signal splitting were done in software. Random noise added by separate well-isolated hardware stages is not correlated. Also if the signal is split in hardware, then the system noise level can be checked by firing plasma shots with the receiver horn covered and cross correlating/autocorrelating as appropriate. The measured correlated signal under these conditions represents the intrinsic noise correlation level of the system, and should not be (as discussed above) the measurement limit of the system. That is we require the correlated signal under these conditions to be $\ll 10^{-3}$ of the correlated signal with the system exposed to the plasma.

A. Viewing system

The selection of a horn to couple the free space radiation to the waveguide for transport to the heterodyne receiver requires a design that provides adequate spatial resolution inside the emitting plasma volume. The radiation pattern of a standard horn usually subtends a large solid angle making a typical spot size in the plasma of about 5 cm. Utilizing Gaussian optics²³ a horn-lens system can be used to form a viewing beam with a waist in the plasma, defining the viewing geometry (Fig. 7). Only radiation originating within the

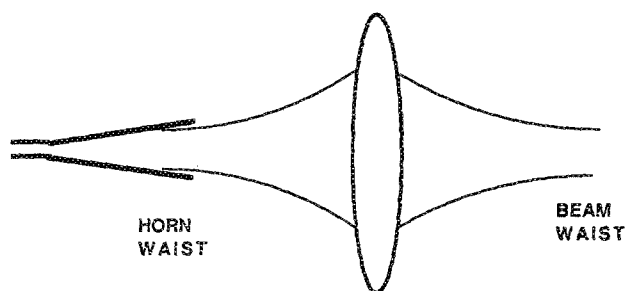


FIG. 7. Gaussian beam optics showing horn waist, focusing lens, and beam waist.

beam contours enters the horn. We propose to view horizontally from the outside of the machines. The selection of the beam parameters will be governed by the desire to maintain Gaussian purity, maximize power flow through the vacuum port, and attain minimum spot size in the plasma. A corrugated conical horn and a lens or focusing mirror will be designed to couple efficiently to the viewing beam while providing broadband 80–110 GHz performance by matching the frequency scaling of the horn with that of the beam. The horn/lens will view the plasma through a wedged quartz vacuum window located on a horizontal port. An oppositely oriented, wedged Teflon piece will be added in order to compensate for beam deflection due to the quartz vacuum window. Beam dumps will not be required since we will be detecting optically thick emission.

Delivery of the radiation from the machine to the receiver will be accomplished using C-band, over-moded waveguide. Fundamental waveguide sections immediately after the horn provide polarization selection prior to transmission by the oversized section. Then H -plane, quasioptical 90° C-band bends give the necessary direction changes with minimal loss. A waveguide high pass filter is provided to eliminate the lower mixer sideband. A schematic of the viewing system is shown in Fig. 5.

B. Receiver

The configuration for 2-Tesla operation consists of a mixer with an intermediate frequency (IF) output of 2–18 GHz. The local oscillator (LO) frequency will be in the range 80–90 GHz and the system will be in WR-10 waveguide. The coaxial IF system consists of two low noise IF amplifiers each with 30-db gain, providing input to an eight-way power division network (7-db loss per channel). The filter bank system offers simultaneous information at all frequencies of interest; thus, a spectrum is available with each sampling. Using a fixed frequency, phase-locked, Gunn local oscillator makes for a quiet receiver easily calibrated with LN_2 . Simplicity, reliability, and cost are also attractive features.

Frequency resolution will be provided by a filter bank consisting of eight bandpass filters for each IF amplifier. We will have an array of fixed filters with different channel center frequencies and bandwidths, each one optimized for a particular plasma radius and range of expected electron temperatures at 2 Tesla. There will also be a set of variable center frequency, YIG-tuned, bandpass filters that will allow us to vary the separation between channels for cross-channel correlation experiments. Video crystal detectors with a sensitivity of 0.5 mV/ μW and video amplifiers provide signals to the data acquisition. A standard 12-bit, 1–5 MHz, CAMAC-based data acquisition system will be used (e.g., Lecroy Model 6810 ADC). A schematic of the receiver is shown in Fig. 6.

V. DISCUSSION

From the considerations discussed above and our design efforts on this problem to date, we believe it is reasonably likely that turbulent temperature fluctuations \tilde{T}_e/T_e

$\approx 2 \times 10^{-3}$ with wavelengths greater than 1.5 cm can be measured on ATF and TEXT for frequencies less than ≈ 100 kHz. On higher field, higher temperature, longer pulse devices it is likely that considerably better resolution can be achieved. We hope to demonstrate the likely resolution on ATF and TEXT in less than two years.

ACKNOWLEDGMENTS

This work is in support of the United States Department of Energy Office of Fusion Energy Transport Initiative and involves a collaborative effort between Auburn University, the Georgia Institute of Technology, the University of Texas at Austin, and Oak Ridge National Laboratory.

¹L. A. Artsimovich, Nucl. Fusion **12**, 215 (1972).

²H. P. Furth, Nucl. Fusion **15**, 487 (1975).

³P. C. Liewer, Nucl. Fusion **25**, 543 (1985).

⁴A. Cavallo, H. Hsuan, D. Boyd, B. Grek, D. Johnson, A. Kritiz, D. Mikkelsen, B. LeBlanc, and H. Takahashi, Nucl. Fusion **25**, no. 3 (1985).

⁵D. Boyd, F. Stauffer, and A. Trivelpiece, Phys. Rev. Lett. **37**, no. 2 (1976).

⁶Sillen, Pickaar, Oyevaar, Gorbunov, Bagdasarov, and Vasin, Nucl. Fusion **26**, no. 3 (1986).

⁷V. Arunasalam, R. Cano, J. Hosea, and E. Mazzucato, Phys. Rev. Lett. **39**, no. 14 (1977).

⁸A. Cavallo and R. Cano, Plasma Phys. **23**, 61 (1981).

⁹G. Bell, R. Gandy, J. Wilgen, and D. Rasmussen, Rev. Sci. Instrum. **59**, 1644 (1988).

¹⁰D. Brower, W. Peebles, N. Luhmann, and R. Savage, Phys. Rev. Lett. **54**, 689 (1985).

¹¹B. Carreras (private communication, 1989).

¹²A. Bhattacharjee *et al.*, Phys. Fluids **26**, 880 (1983).

¹³B. Carreras, viewgraphs from oral presentation, ORNL, May 2, 1990, and private communication 6/21/90.

¹⁴M. Bornatici, R. Cano, O. DeBarbieri, and F. Engelman, Nucl. Fusion **23**, 1153 (1983).

¹⁵G. Bekefi, *Radiation Processes in Plasmas* (Wiley, New York, 1966), p. 330.

¹⁶C. E. Thomas, Jr., "Using Crossed-Sightline Correlation of Electron Cyclotron Emission to Measure Magnetic Fluctuations in Plasmas," EC6-Joint Workshop on ECE and ECRH, Sept. 16-17, 1987, Oxford, UK, proceedings.

¹⁷C. E. Thomas, Jr., G. R. Hanson, R. F. Gandy, D. B. Batchelor, and R. C. Goldfinger, Rev. Sci. Instrum. **59**, 1990 (1988).

¹⁸G. R. Hanson and C. E. Thomas, Jr., Rev. Sci. Instrum. **61**, 671 (1990).

¹⁹P. Efthimion, Oral presentation, Transport Workshop, Fusion Research Center, Univ. of Texas, Austin, Texas, January, 1989.

²⁰G. L. Bell, R. F. Gandy, J. B. Wilgen, and D. A. Rasmussen, "ECE Radiation Path Design for ATF," Auburn University Physics Report PR21, Technical Report MMESI-19x-5596V-2, October, 1987.

²¹J. S. Bendat and A. G. Piersol, *Random Data: Analysis and Measurement Procedures*, 2nd ed. (Wiley Interscience, New York, 1986).

²²R. Loudon, *The Quantum Theory of Light*, 2nd ed. (Oxford University Press, New York, 1983).

²³Kogelnik and Li, Appl. Opt. **5**, 1550 (1966).

²⁴M. Born and E. Wolf, *Principles of Optics*, 6th ed. (Pergamon, New York, 1980).